Effect of welding heat input on microstructure and residual stresses of duplex stainless steel welds

N. Ouali[a,b], K. Khenfer[b], B. Belkessa[a] , B. Cheniti[a]

[a] Research Center in Industrial Technologies, CRTI,
P.O. Box 64, 16014, Cheraga, Algiers, Algeria

[b] LSGM, FGMGP, USTHB, 16111 Algiers, Algeria

n.ouali@crti.dz

Abstract:

In the present investigation, the influence of heat input on phase balance, microstructure and residual stresses of lean duplex stainless steel welds are discussed. The weldments were made with different heat inputs through changes in welding current and travel speed, using tungsten inert gas process. The microstructural evolution was characterized using optical and scanning electron microscopy, while the ferrite content was estimated using a Fischer ferritescope instrument and the residual stresses were measured on surface by X-ray diffraction technique. The experimental results show significant changes in microstructure and ferrite content with a large fraction of reformed austenite also, the samples exhibit compressive residual stresses on the superficial layers of the weld.

Keys words: Lean duplex stainless steel, Welding heat input, Residual stresses, X-ray diffraction

1. Introduction:

Dual phase stainless steels are the most popular materials used over the last thirty years, where high mechanical strength and high corrosion resistance are required. This material satisfies these requirements as in oil and gas industry, pressure vessels and chemical transport [1]. The microstructure of this alloy consists in ferrite and austenite phases in equal proportions, to provide and combine the properties of austenitic and ferritic stainless steels [2]. The main elements which compose these steels are chromium molybdenum, nickel and manganese. Owing of the high cost of nickel, the lightened range as lean duplex stainless steels (LDSSs) have been developed enabling partial or complete replacement of expensive Ni used [3]. As a result, grades such as S30403 and S31603 were elaborated as well as S32101 (LDX 2101) one, which is the most popular lean duplex stainless steel, widely used in steam generators and pressure vessel [4]. It provides both superior mechanical strength and greater chloride stress corrosion cracking resistance [5]. The fields where this grade is used regularly develop, having real effects on both economy and ecology. The present work is an attempt to study this material experimentally in welding conditions by varying energy to describe their effect on phase balance and residual stresses evolution of LDX 2101 lean duplex stainless steel welds.

2. Materials and methods:

2.1. Weld specimens:

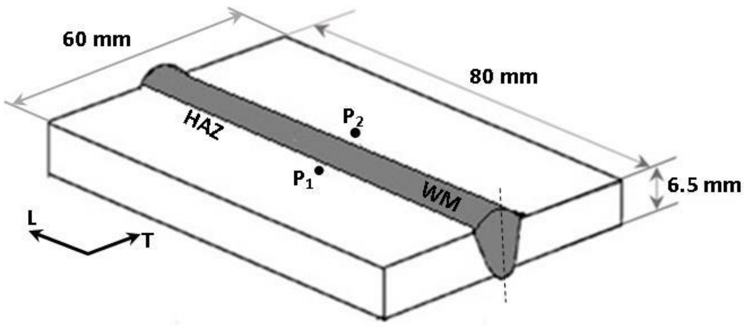

Fig.1: Weld design with residual stresses measurements locations

The base metal used in this work was a lean duplex stainless steel, LDX 2101(UNS S32101). The material was received in a plate form of 6.5 mm thickness and dimensions of 80x60mm². A multipass gas tungsten arc welding process (GTAW) was employed to join the specimens, using a duplex stainless steel electrode (ER2209). The chemical composition of base and filler metal, is reported in Table 1. A single V groove with an angle of 60° was prepared with particular attention to remove impurities from the joint edges.

During welding process, two levels of heat input were used by varying welding current from 80A (**W1**) and 130A (**W2**). Welding heat inputs were calculated according to the following equation:

$$Heat\ input = \eta * \frac{I*U}{S*100} \qquad (kJ/mm) \qquad eq.1$$

Where I is the welding current (A), U is the applied voltage (V), η* is the arc efficiency of the welding process taken as 70% for the GTAW process [6] and S is the welding speed (mm/s) manually measured.

In order to observe the microstructural evolution that occurs during welding, metallographic sections transverse to the welding direction were prepared and etched with Beraha reagent (0.7 g $K_2S_2O_5$, 20 ml HCL, and 80 ml H_2O). The ferrite volume fraction was estimated using a Fischer ferritescope (MP30E); this instrument measures the ferrite content using the magnetic permeability of steels.

The residual stresses were measured by XRD, using a four-circle XRD 3003 PTS Seifert goniometer with Cr-Kα radiation as X-ray source, which wavelength k = 2.289 Å. The voltage and current were 40 kV and 30 mA. The diffraction angle 2θ ranges from 149° to 161°. The measurements were made on the {211} atomic plane of the studied material at 2θ= 156.105°.

The residual stress analysis was carried out on the basis of the $\sin^2\psi$ method, which is employed for polycrystalline materials and several types of Welding process.

Table 1: Chemical composition of the base and filler metals in wt.(%).

Alloy element	*C*	*Mn*	*Si*	*Cr*	*Ni*	*P*	*Cu*	*Mo*	*N*
Base metal (S32101)	0.043	4.72	0.702	21.2	1.74	0.024	0.246	0.297	0.253
Filler metal (ER2209)	0.03	1.0	0.90	21.8	6.8	0.026	0.01	3.1	0.15

Table 2: Parameters used during welding process

Specimen	*Welding pass n°*	*Welding current (A)*	*Welding voltage (V)*	*Average heat input per pass (kJ/mm)*
W1	1st	80	8.25	1.52
	2nd	80	8.25	1.21
	3rd	80	8.75	0.96
W2	1st	130	10.75	1.93
	2nd	130	11.25	1.35
	3rd	130	12	1.08

2.2. X-ray method for residual stress analysis:

The XRD method employs Bragg's theory (eq.2) to evaluate the residual strains then the residual stresses present in the atomic plans, relating the crystallographic lattice spacing characterized by Miller indices hkl [7,8].

$$2d_{hkl}\sin\theta_{hkl} = n\lambda \qquad eq. 2$$

Where, d_{hkl} is the spacing between two crystal lattices and λ is the wave length of X ray, θ_{hkl} is the angle between the incident X-ray and the scattering plane, and n is an integer number (diffraction order) as shown in Fig.2.

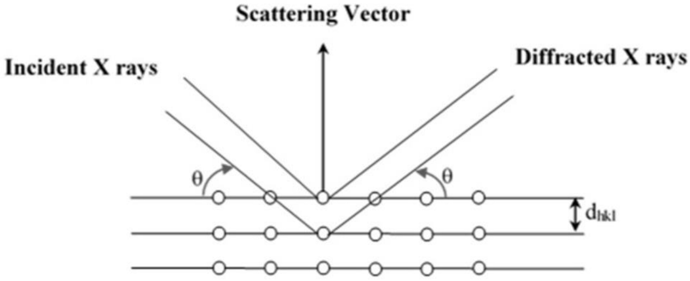

Fig. 2: Illustration of Bragg's theory for a crystal lattice.

To get strains measurements, the sample is positioned in the X-ray diffractometer, and is exposed to an X-ray beam that interacts with the crystal lattice to result in diffraction patterns. In the presence of residual stresses, this leads to a small change in the lattice spacing (Δd_{hkl}), which causes a corresponding shift in the diffraction angle $\Delta\theta_{hkl}$.

$$\Delta\theta_{hkl} = -tan\theta_{hkl} * \frac{\Delta d_{hkl}}{d_{hkl}} \qquad eq. 3$$

The strains measurements are based on Hook's low (elasticity's theory) [9], so for any deformation in arbitrary direction, the strain ε is expressed as follow (eq.3):

$$\varepsilon_{hkl} = \frac{d_{hkl} - d_{0,hkl}}{d_{0,hkl}} = -\frac{1}{2}\Delta 2\theta_{hkl} * cot\theta_{0,hkl} \qquad eq. 4$$

Where d_{hkl} and d_0 are strained and reference lattice parameters respectively.

3. Results and discussion:

3.1 Microstructural analysis and Ferrite content:

The microstructure of Lean DSS (LDX 2101) base metal is shown in Fig. 3. The optical micrograph reveals a two-phase banded structure, typical feature of rolled duplex stainless steels, with near equal proportions of austenite and ferrite. The austenite phase (γ) appeared as discontinuous white grains, while the brown (dark) region is the ferrite phase (δ) with continuous morphology. This base material contains 48% of ferrite and 52% of austenite**.**

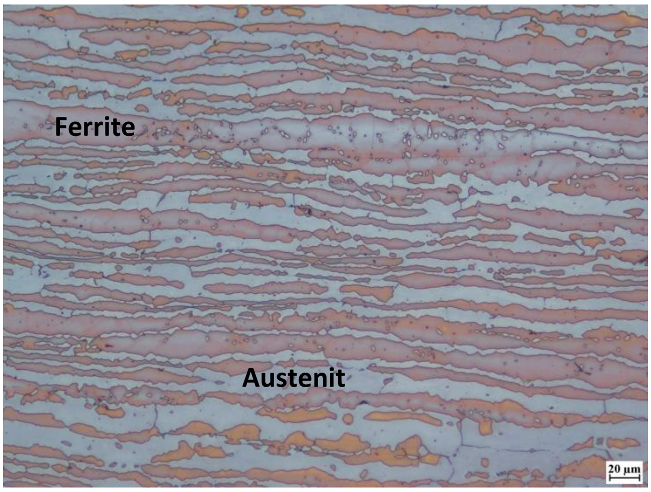

Fig. 3: Optical micrograph of LDX 2101 base metal

.

Microstructural analysis of the LDX 2101 of fusion boundary and HAZ as shown in Fig. 4 revealed that the weld region contained more austenite than the HAZ and parent material. The solidification mode is fully ferritic as the Cr_{eq}/Ni_{eq} ratio is greater than 1.95 [11], the microstructure is characteristic for the welded duplex SSs which consist of δ-ferrite phase and reformed austenite phase.

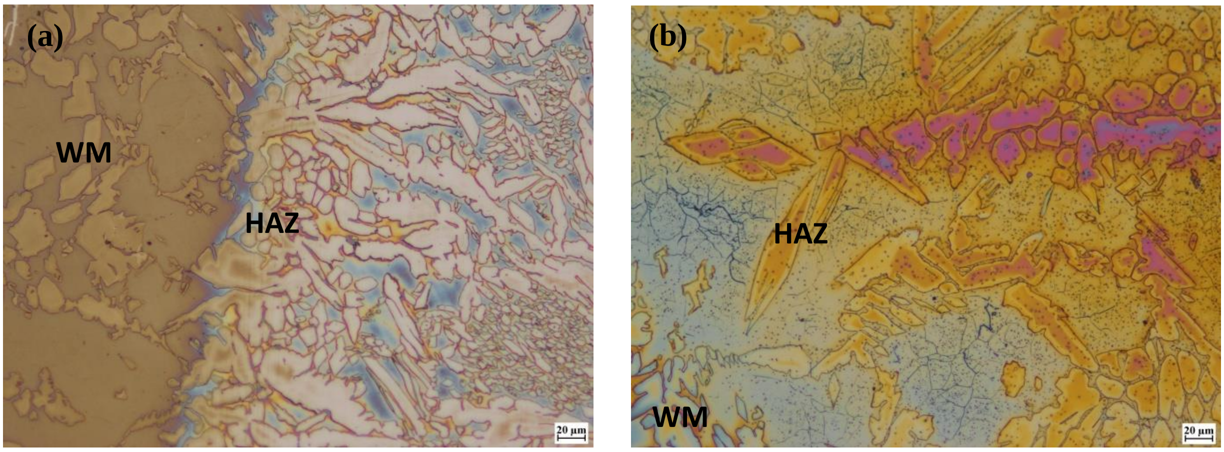

Fig. 4: Optical micrographs showing the microstructure of the weld region and heat affected zone for the heat inputs: a) W1, b) W2,

In the HAZ, the microstructure evolution and the austenite reformation depends upon the chemical composition and the cooling rate [12] which is dictated by the welding parameters and the material geometry [13]. The SEM micrographs illustrated by Fig. 5, exhibit practically the same microstructure as the weld zone, but show an important grain coarsening. The HAZ is very narrow, about 180µm in width, with higher cooling the austenite reformation is relatively slowed and higher ferrite content is observed.

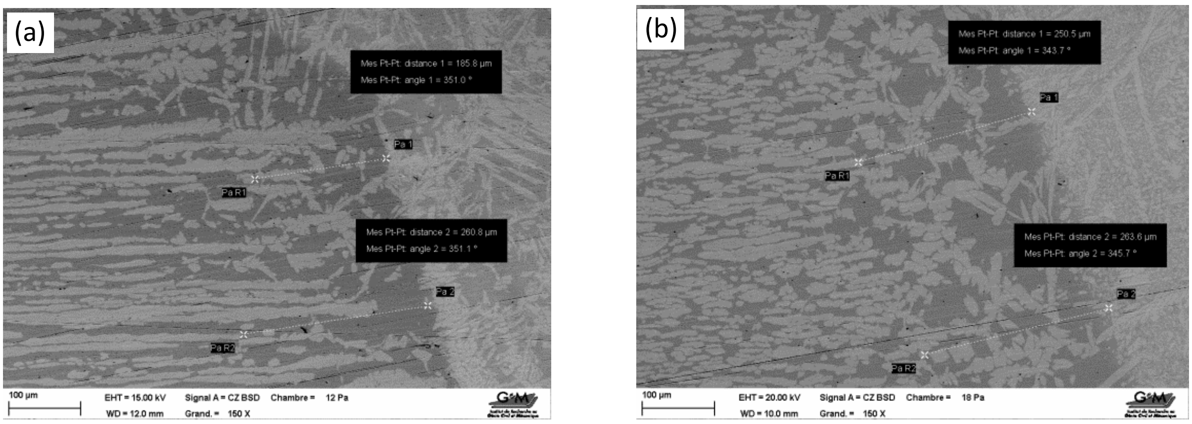

Fig. 5: SEM images of the HAZ adjacent to the fusion boundary of LDSS welds: a) W1, b) W2.

Table.3: The measured austenite and ferrite content using ferritoscope instrument

Phase(%)	*BM*	*W1*		*W2*	
		WM	HAZ	WM	HAZ
Austenite	52	55	30.9	66.5	38.2
Ferrite	48	45	69.1	33.5	61.8

The results listed in Table 3 for each sample showed a higher fraction of austenite than ferrite in the weld metals. This large amount of γ-austenite in WMs is attributed to the high Ni content in the filler metal ER 2209 (6.8 wt.) and the large transformation time of δ-ferrite to austenite γ.

3.2 Residual stress evolution:

The XRD method does not measure stresses directly but measures strains from which stresses values are calculated for tow directions (L and T). The longitudinal and transverse RS on the weld surface for the samples locations were all compressive as presented in Table 4. In the same time, they are higher in the longitudinal direction than in the transverse one. This result is explained by the restrained and unrestrained cooling phenomena which take different directions along and perpendicular to the weld seam respectively.

Table.4: Distribution of longitudinal and transverse residual stresses on samples top surface

Sample	*Location*	σ_L *(MPa)*	σ_T *(MPa)*
W1	P_1	-276	-165
	P_2	-292	-178
W2	P_1	-226	-166
	P_2	-208	-241

4. Conclusion:

The general conclusion deriving from above for 6 mm thick lean duplex stainless steel welds made by different welding energy, can be summarized in the following points:

-The microstructure revealed fully penetrated welds with no precipitation of carbides in the weld area and in the HAZ for the three heat input modes.

-Due to its effect on the weld thermal cycle, the heat input has been shown to have a significant influence on the phase balance of the welded lean duplex stainless steel, where the austenite content increases with heat input increases.

-The welding heat input has a great effect on residual stresses, the weld superficial residual stresses measured by mean of $\sin^2\psi$ method shows a compressive character, while they decrease as the heat input increases.

5. References

[1] D. J. K. John C. Lippold, “Welding Metallurgy and Weldability Of Stainless Steels.” 2005.

[2] R. Gunn, “Duplex Stainless Steels: Microstructure, Properties and Applications,” *Abingt. Publ.*, p. 219, 1997.

[3] J. Han, J. P. Sun, Y. Han, and H. Liu, “Hot workability of the as-cast 21Cr economical duplex stainless steel through processing map and microstructural studies using different instability criteria,” *Acta Metall. Sin. (English Lett.*, vol. 30, no. 11, pp. 1080–1088, 2017.

[4] Z. Brytan and J. Niagaj, “Microstructural Characterization of Lean Duplex Stainless Steel UNS S32101 Welded Joints Using Electron Backscatter Diffraction,” *Chiang Mai J. Sci.*, vol. 40, no. 5, pp. 923–937, 2013.

[5] J. Pilhagen and R. Sandström, “Influence of nickel on the toughness of lean duplex stainless steel welds,” *Mater. Sci. Eng. A*, vol. 602, pp. 49–57, 2014.

[6] S. Jana, “Effect of heat input on the HAZ properties of two duplex stainless steels,” *J. Mater. Process. Technol.*, vol. 33, no. 3, pp. 247–261, 1992.

[7] B. L. Adams, “Handbook of Material Charecterisation,” *Asm*, vol. 10, p. 1310, 1998.

[8] N. Syahida, M. Nasir, M. Khairul, A. Abdul, S. Mamat, and M. Iqbal, “Review on Welding Residual Stress,” *ARPN J. Eng. Appl. Sci.*, vol. 11, no. 9, pp. 6166–6175, 2016.

[9] V. I. Monin, R. T. Lopes, J. T. De Assis, N. Friburgo, and R. De Janeiro, “after Welding of Duplex Stainless Steel Plates,” *Mater. Res.*, vol. 17, pp. 64–69, 2014.

[10] S. Kumar and A. S. Shahi, “Effect of heat input on the microstructure and mechanical properties of gas tungsten arc welded AISI 304 stainless steel joints,” *Mater. Des.*, vol. 32, no. 6, pp. 3617–3623, 2011.

[11] Z. Brytan, J. Niagaj, and Reiman, “Corrosion studies using potentiodynamic and EIS electrochemical techniques of welded lean duplex stainless steel UNS S82441,” *Appl. Surf. Sci.*, vol. 388, pp. 160–168, 2016.

[12] Y. T. Shin, H. S. Shin, and H. W. Lee, “Effects of heat input on pitting corrosion in super duplex stainless steel weld metals,” *Met. Mater. Int.*, vol. 18, no. 6, pp. 1037–1040, 2012.

[13] E. M. Westin, *Welds in the Lean Duplex Stainless Steel LDX 2101 Effect of Microstructure and Weld Oxides on corrosion properties Microstructure and properties of welds in the lean duplex stainless steel LDX 2101*, Royal Inst. 2008.